ISSN 1330-3651 (Print), ISSN1848-6339 (Online) https://doi.org/10.17559/TV-20200714151347
Original scientific paper

CFD Evaluation of a New Centrifugal Pump Concept for Rocket Propulsion

Malael ION*, Bucur IOANA

Abstract: The rocket propulsion system provides forces to a flight shuttle so that it can accelerate or decelerate and overcome the drag force or change direction. The simplest propulsion system can be made using pressurized propellant tanks with supply of compressed gas but, for minimum weight design requirements, a system with propellant pumps satisfies better. This paper aims to evaluate the performances of a new centrifugal pump concept using computational fluid dynamics. The paper is based on an innovative pump design consisting of two centrifugal stages superposed into a novel and promising configuration. The CFD analysis is performed on 3D domains by using the CFD commercial code ANSYS CFX. The numerical solvers used are pressure based using the SIMPLE method with RANS. The post processing of the results delivers speed, pressure and temperature distribution in the field. A classic two stage centrifugal pump is compared with the new stage-over-stage design, where the axial length is considerably reduced. Regarding the total efficiency, in both cases its value is around 97%. This paper presents an innovative geometry for centrifugal pumps, that can contribute to the improvement of rocket propulsion systems.

Keywords: centrifugal pump; computational fluid dynamics; rocket propulsion; stage-over-stage

1 INTRODUCTION

Current state of the art regarding centrifugal pumps highlights their wide range of application, including not only industrial uses, but also residential ones. Different designs for centrifugal pumps are available, according to their domain of use, which includes irrigation, stream power plants, oil refineries, hydraulic power service and aerospace engineering [1]. Such designs include mixed flow pumps, as studied in [2] or multi-stage multiphase pumps, as analyzed by J. Zhang et. al. in paper [3], with emphasis on their characteristics and flow behaviour at different operating conditions. Due to the expansion of their applications, from propulsion of marine devices [4] to hydraulic applications and medical devices, the performances and working ranges of centrifugal pumps should be carefully assessed prior to their manufacturing. Thus, computational fluid dynamics simulations regarding the flow through such a pump are becoming more and more relevant. Such studies provide an insight into the flow characteristics that can help in the optimization process. The importance of the advantages provided by computational fluid dynamics simulations in the field of turbomachinery are highlighted in [5].

The development of centrifugal pumps in the aerospace industry focuses mainly on obtaining pumps with a wider stable performance map so that they can be successfully used for designing rocket engines. Design concepts that improve flow range of pumps in rocket engines include different casing treatments and also limitations on hydraulic loadings within the blading, which are meant to decrease chances of surge or delay it [6].

Liquid-propellant propulsion systems, such as rocket engines, demand that the initial pressure of the propellants is sufficient to surpass eventual losses in order for it to reach the combustion chamber at an optimal pressure. This is necessary for the combustion process to be stable. In order to gain the needed pressure, the relevant solutions would be pressure-fed systems and pump-fed systems [7]. Pressure-fed engines can be based on self-pressurization or pressurization by another foreign high pressure gas. Pump-fed engines operate under the principle of a turbo-charger to achieve the pressurization of the propellants. The last ones are preferred due to their light weight and innovative perspectives [8].

Rocket engines that use fully cryogenic propellants, such as liquid oxygen or liquid hydrogen, are currently preferred in the industry of rocket science development. Hence, it is required to examine the behaviour of centrifugal pumps pressurizing such fluids in order to determine precautions that must be taken into consideration. The most common issue when using semi-cryogenic or cryogenic propellants is that the process of their pressurization can lead to cavitation conditions exposure [9]. There are many papers concerning the cavitation phenomenon, which analyze it and try to predict the characteristics of the flow, as well as to give relevant solutions to prevent it [10-12]. Cavitation represents the main cause of instability in pumps according to [13]. This phenomenon causes cavities to form in the flow due to the fact that the local static pressure approaches the fluid vaporization pressure [6]. Therefore, to avoid cavitation, pumps are designed to function below cavitation conditions by using an inducer and so the system performance is improved [14]. The inducer proceeds in increasing the static pressure of the fluid that enters the pump to a value that allows the main impeller of the pump to function normally [15]. An innovative geometry that might improve cavitation resistance is the centrifugal vortex pump concept, developed by Mihalić et al. [16].

In order to achieve pumps that work more efficiently, reliably and quietly at lower cost, pump designers are exploiting modern methods, such as numerical simulations, that allow the prediction of flow behaviour in different machines before manufacturing them. These can be carried out using CFD software. Such software allows the designer to have a wider understanding regarding the flow phenomenon in the centrifugal pump and therefore, to correct the design in order to achieve better performances [17]. Often, the numerical results are compared with experimental data in order to validate different CFD methods [18].

Further on, a new geometry design for centrifugal pumps is proposed and its performances are evaluated by employing CFD numerical simulations. The proposed

design contributes to the development and improvement of rocket propulsion systems.

2 METHODOLOGY

In this section aspects regarding the generation of the two geometries are discussed, as well as the methods used for the CFD numerical simulations. Furthermore, grid production features are explained and the case set-up for the investigated geometries in ANSYS CFX is detailed.

2.1 Centrifugal Pump Design

Firstly, a pre-design mathematical model is presented for the assessment of the main design features of the classic two stage centrifugal pump and the proposed stage-over-stage geometry. As input parameters, the pump's mass flow, Eq. (1), and its discharge pressure, Eq. (2) are established in accordance with the pump's application [19].

$$\dot{Q} = \rho v A \tag{1}$$

$$p_d = p_s + (\Delta p)_{pump} \tag{2}$$

where $\dot{Q}$ is the pump's mass flow the quantity of fluid going through the discharge per unit time, ρ air density, v velocity, A area, p_d discharge pressure, p_s suction pressure and Δp the pressure difference.

As discussed in the introduction, the cavitation phenomenon is unwanted and in order to avoid it NPSHa (available net positive suction head) should be greater than NPSHr (required net positive suction head) [20]. NPSHa represents a monitor for the absolute pressure at the inlet, while NPSHr signifies the limit value of the head. The expression for the head, that describes the pressure increase provided by the centrifugal pump between the processes of discharge and suction, is evaluated using Eq. (3):

$$\Delta H = \frac{p_d + p_s}{\rho g} + Y_s + Y_d \tag{3}$$

where ΔH is the head, calculated as a function of discharge pressure (p_d), suction pressure (p_s), air density (ρ), acceleration of gravity (g), losses at suction (Y_s) and losses at discharge (Y_d).

The impeller's diameter (D_2) can be calculated as a function of specific diameter (D_s), Eq. (4), or angular speed (ω) and velocity at impeller's outlet (u_2), Eq. (5):

$$D_2 = \frac{D_s \sqrt{\dot{Q}}}{(g\Delta H)^{\frac{1}{4}}} \tag{4}$$

$$D_2 = \frac{2u_2}{\omega} \tag{5}$$

The relative angles and velocity components (c - absolute velocity, w - relative velocity) are determined from the velocity triangles as explained in [20]. For the impeller inlet the following equations are employed:

$$c_1 = \frac{\dot{Q}}{\rho A_1} \tag{6}$$

$$u_1 = 2\pi n D_1 \tag{7}$$

$$w_1 = \frac{c_1}{\sin(\beta_1)} \tag{8}$$

where c_1 is the inlet absolute velocity, u_1 the velocity at impeller's inlet, n the rotational speed, D_1 the inlet's diameter, w_1 the inlet relative velocity and β_1 the inlet relative angle.

Whereas for the impeller outlet the following equations apply:

$$c_2 = \sqrt{c_{2m}^2 + c_{2u}^2} \tag{9}$$

$$w_2 = \sqrt{\left(c_2^2 + u_2^2\right)\left[2u_2 c_2 \cos(\alpha_2)\right]} \tag{10}$$

where c_2 is the outlet absolute velocity, c_{2m} is the meridional component of the outlet absolute velocity, c_{2u} is the tangential component of the outlet absolute velocity, w_2 is the outlet relative velocity and α_2 the outlet absolute angle.

The relative (β_2) and absolute (α_2) angles at outlet are calculated using Eq. (11) and Eq. (12) respectively:

$$\beta_2 = \arctan\left(\frac{c_{2m}}{u_2 - c_{2u}}\right) \tag{11}$$

$$\alpha_2 = \arctan\left(\frac{c_{2m}}{c_{2u}}\right) \tag{12}$$

The number of blades and their height at the outlet were determined using the following formulations:

$$z = 6.5 \frac{D_2 + D_1}{D_2 - D_1} \sin(\beta_1 - \beta_2) \tag{13}$$

$$h_2 = 0.78\left(\frac{N_s}{100}\right)^{\frac{1}{6}} \sqrt{\frac{\dot{Q}}{n}} \tag{14}$$

where z is the number of blades, h_2 their height and N_s the specific speed for the pump.

As for the impeller efficiency evaluation, the next three equations were used.

$$Power_{inlet} = \frac{2\pi NT}{60 \times 1000} \tag{15}$$

$$Power_{outlet} = \frac{(p_d - p_s)Q}{1000} \tag{16}$$

where N is rotational speed, T is the shaft torque and Q is the flow rate.

$$Efficiency = \frac{Power_{outlet}}{Power_{inlet}} \times 100 \quad (17)$$

The pre-design procedure is thoroughly discussed in [19, 21]. The calculated parameters were used in Vista CPD, provided by ANSYS, in order to generate the 3D models for both analyzed geometries. The cross sections for both centrifugal pumps studied in this paper are illustrated in Fig. 1.

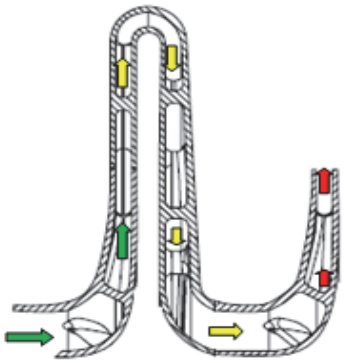

a) Classic two stage

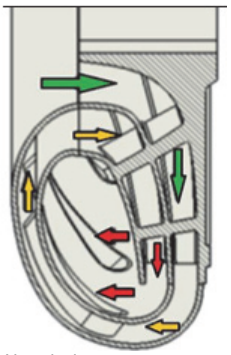

b) New design - stage-over-stage

Figure 1 Centrifugal pump cross section

The green arrows represent the inlet of the centrifugal pump and the outlet is highlighted with red. If in the classic configuration the outlet is well known, in the new design this is through the stator blades. The space between the stator and the rotor from stage 2 will be used to design a volute shape, employed in the discharge process.

2.2 CFD Methods and Models

The Reynolds-Averaged Navier-Stokes (RANS) formulations with the correspondent turbulence closures are very useful in particular for "fast-screening" of a large number of cases or set-ups in Computational Fluid Dynamics (CFD). Steady-state RANS techniques are preferred methods for the analysis of compressible turbulent flows due to the large number of set-ups that can be simulated in a short period of time in order to identify trends in the flow behaviour [22-24].

Within the RANS method, two-equation turbulence models are largely used. Probably the most popular two-equation model is the standard k-ε model [25], which is robust, fast and gives reasonable accuracy for a wide range of turbulent flows. Another two-equation model is the standard k-ω turbulence model, which is based on Wilcox's k-ω model [26]. An improved turbulence model is Menter's Shear Stress Transport (SST) k-ω model [27] with compressibility effects, for which the two-equations for turbulent kinetic energy and specific turbulent kinetic energy dissipation rate are given in Eq. (18).

$$\begin{aligned}
&\frac{\partial k}{\partial t} + \bar{u}\frac{\partial k}{\partial x} + \bar{v}\frac{\partial k}{\partial x} + \bar{w}\frac{\partial k}{\partial x} = \Gamma_k\left(\frac{\partial^2 k}{\partial x^2} + \frac{\partial^2 k}{\partial y^2} + \frac{\partial^2 k}{\partial z^2}\right) + \tilde{G}_k - Y_k \\
&\frac{\partial \omega}{\partial t} + \bar{u}\frac{\partial \omega}{\partial x} + \bar{v}\frac{\partial \omega}{\partial x} + \bar{w}\frac{\partial \omega}{\partial x} = \Gamma_\omega\left(\frac{\partial^2 \omega}{\partial x^2} + \frac{\partial^2 \omega}{\partial y^2} + \frac{\partial^2 \omega}{\partial z^2}\right) + \\
&+G_\omega - Y_\omega + D_\omega
\end{aligned} \quad (18)$$

where: k is turbulent kinetic energy; ω is specific turbulent kinetic energy dissipation rate; Γ_k, Γ_ω are effective diffusivities for k and ω; $\widetilde{G}_k$ represents the production of turbulence kinetic energy; G_ω represents the production of ω; Y_k and Y_ω represent the dissipation of k and ω and D_ω represents the cross-diffusion term.

Using the commercial solver CFX (ANSYS, Inc.), the two-equation SST turbulence model was used for the investigation of the compressible flow in a new liquid hydrogen centrifugal pump design. A comparison between this new pump design and a classic two-stage centrifugal pump was carried out in this paper. The geometries for the two cases are the ones illustrated in Fig. 1.

2.3 CFD Set-up

In order to prepare the geometries for the numerical simulations, for both cases the computational domain was realized using the TURBOGRID software, which is an automatic block-structured meshing system devoted to rotating machinery configurations.

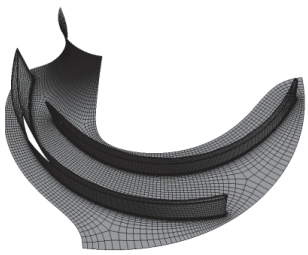

a) Impeller 1

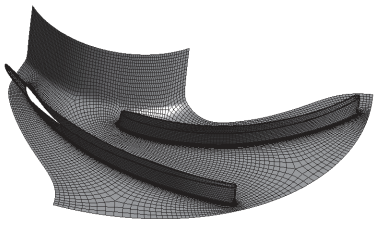

b) Impeller 2

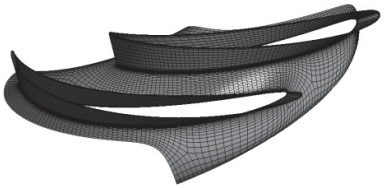

c) Stator

Figure 2 Grids for the components of the centrifugal pump

In the mesh generation process the mesh's quality, in terms of orthogonal, expansion ratio and cell aspect ratio were considered. The generated meshes for impeller 1, impeller 2 and stator are illustrated in Fig. 2.

The target for the final mesh size was about 1.5 million grid cells for all domains, with a normal blade count of about 30. The first inner cell size was defined in order to reach the unit value for $y+$ at the first point away from the solid walls.

Regarding the set-up of the two investigated cases, using both discussed geometries, at the inlet, the total pressure $p_{in} = 20$ bar is set up to avoid problems regarding the cavitation phenomenon. Usually, to reach this pressure an inducer can be used but in this paper we investigate only the impeller and stator part and suppose that in each case the outlet pressure from the inducer is 20 bar . At the pump's outlet, the mass flow rate for all sectors was imposed $\dot{Q} = 40.4$ kg/s , and a monitor point at the inlet with this variable was set up to check the convergence of the numerical solution. The walls (blades, hub and shroud) are non-slip, and the moving reference frame model is assigned with rotational speed of 36000 RPM around the Z axis. The turbulent option at the inlet and outlet boundaries is set to medium intensity equal with 5%. The boundary conditions discussed earlier, are illustrated in Fig. 3 and summarized in Tab. 1.

Table 1 Boundary conditions

INLET	$p_{in} = 20$ bar
OUTLET	$\dot{Q} = 40.4$ kg/s

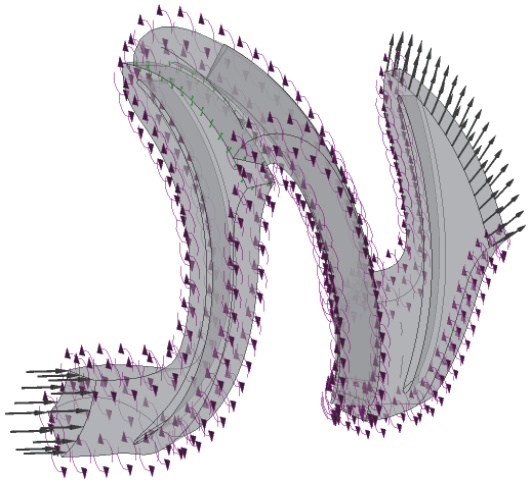

a) Classic two stage

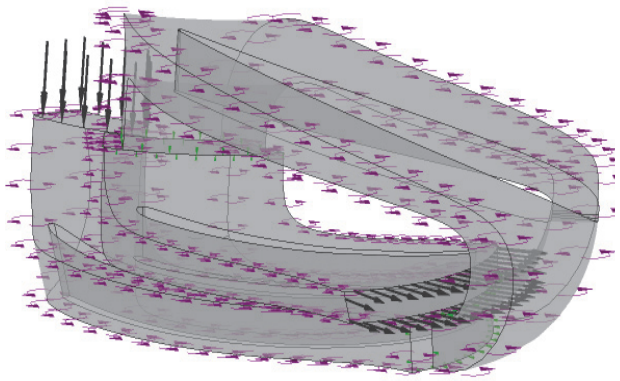

b) New stage-over-stage design

Figure 3 Boundary conditions

3 RESULTS AND DISCUSSION

A 3D CFD analysis was conducted on a single row of a LH2 centrifugal pump. A comparative study between a classic pump configuration and a new design proposed in this paper, stage-over-stage, has been carried out in order to evaluate their performances. Fig. 4 shows the streamlines in blade to blade view for both cases at 50% blade span. No recirculation zones are developed that can influence the pump's performances, as observed in the mentioned figure.

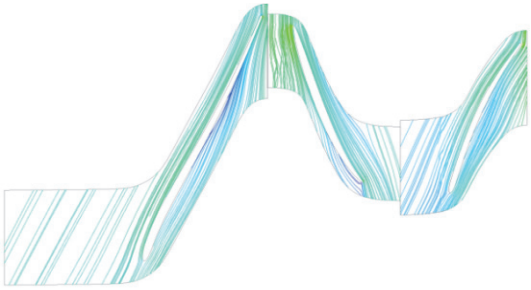

a) Classic two stage

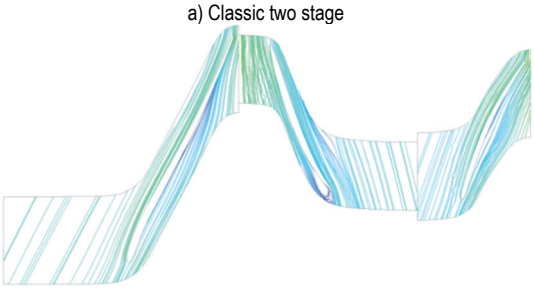

b) New stage-over-stage design

Figure 4 Streamlines at 50% blade span

The existence of liquid hydrogen is conditioned by the temperature conditions. The critical point value so that liquid hydrogen can be formed is below 33 K.

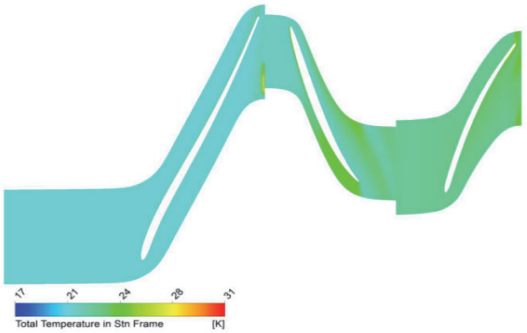

a) Classic two stage

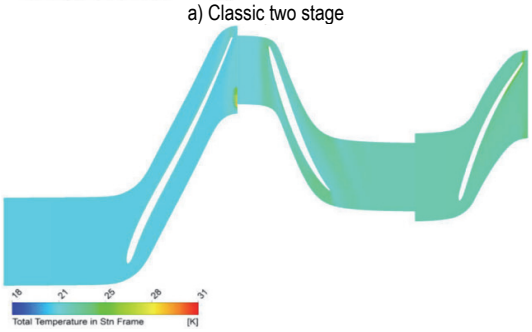

b) New stage-over-stage design

Figure 5 Total temperature in stn frame at 50% blade span

Fig. 5 shows the total temperature in stn (stationary) frame diagrams for each studied case. For both cases the

maximum temperature value is below 31 K so the cooling of the hydrogen below its critical point is assessed in both cases. Furthermore, the lowest value of the temperature is not lower than the freezing point of the liquid rocket fuel. For the proposed stage-over-stage geometry the temperatures are lower overall when compared with the classic two stage configuration, so in real functioning conditions this new design is more reliable, as it is better confined between the freezing limit and the critical point limit of temperature.

To evaluate the pressure in stn frame evolution a meridional view was used to observe the plot on an axial-radial plane. In Fig. 6 are presented the meridional plots for the studied pumps using the circumferential averaging by mass flow option where the total pressure in stn frame value at each sampling point is calculated as a mass flow average over the corresponding circular band.

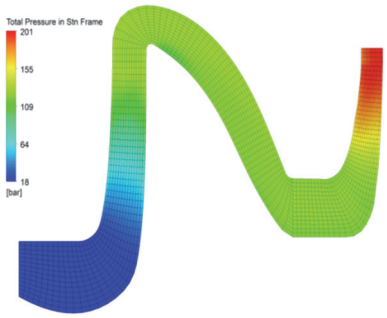

a) Classic two stage

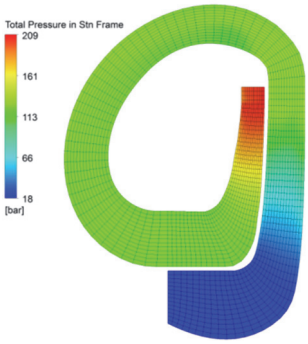

b) New stage-over-stage design

Figure 6 Total pressure in stn frame meridional view

Pressure variation for the studied cases is illustrated from inlet to outlet in Fig. 7.

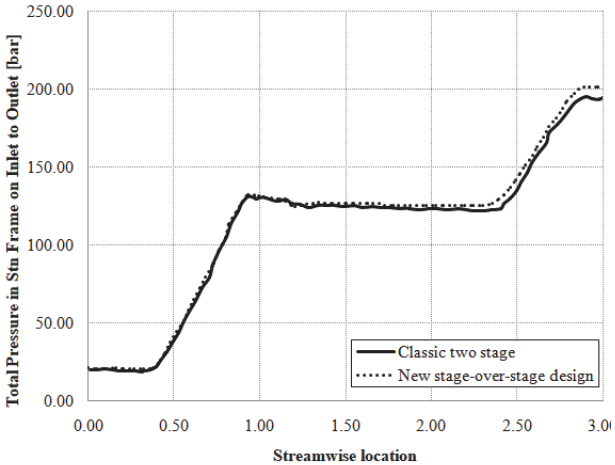

Figure 7 Inlet to outlet pressure stn variation

For both investigated geometries, the pressure outlet values are slightly similar, as can be observed in the two previous pictures.

Furthermore, using Eq. (15), Eq. (16) and Eq. (17), the overall efficiency of the analyzed configurations were approximately 97% for both, the classic two stage and the proposed new design stage-over-stage, centrifugal pumps. The advantage of the proposed geometry is that it reduces by 60% the total axial length of the pump when compared with the classic two stage configuration, without decreasing its performances. On the contrary, it provides better functioning conditions for the liquid hydrogen, regarding its temperature limitations.

4 CONCLUSION

A new design for a radial LH2 centrifugal pump has been investigated using 3D CFD methods. This design consists of an impeller placed over another impeller and in this way the axial length is reduced 60% by comparison with a classic two stages centrifugal pump. With a steady state computational analysis, the performances of these two pumps were evaluated. The total efficiency in both cases is approximately 97%. Within the results, the total pressure at stn frame in meridional view and variation from inlet to outlet was presented. An important aspect of these simulations was related to the temperature value which defines the existence of the liquid hydrogen. By employing the proposed geometry reduced length can be obtained for propulsion systems in the aerospace industry without any efficiency losses, making it a reliable contribution and relevant concept for future research and development projects.

Acknowledgements

This work was carried out within "Nucleu" Program 2N/2019, supported by the Romanian Ministry of Research, Innovation and Digitization.

5 REFERENCES

[1] Thin, K. C., Khaing, M. M., & Aye, K. M. (2008). Design and Performance Analysis of Centrifugal Pump. *World Academy of Science: Engineering and Technology*, *46*, 422-429. https://www.semanticscholar.org/paper/Design-and-Performance-Analysis-of-Centrifugal-Pump-Thin-Khaing/e3510bae5253c090888ac43368b1a136c4b1d2b4

[2] Li, W., Zhang, Y., Shi, W., Ji, L., Yang, Y., & Ping, Y. (2018). Numerical simulation of transient flow field in a mixed-flow pump during starting period. *International Journal of Numerical Methods for Heat & Fluid Flow*, *28*(4), 927-942. https://doi.org/10.1108/HFF-06-2017-0220

[3] Zhang, J., Yongjiang, L., Vafai, K., & Zhang, Y. (2018). An investigation of the flow characteristics of multistage multiphase pumps. *International Journal of Numerical Methods for Heat and Fluid Flow*, *28*(3), 763-784. https://doi.org/10.1108/HFF-06-2017-0252

[4] Milovančević, M., Tijan, E., & Karanikić, P. (2017). Optimization of Vibro-Diagnostic Method for Marine Rotating Pumps. *Technical Gazette*, *24*(3), 703-707. https://doi.org/10.17559/TV-20160208113305

[5] Li, J., Epple, P., Kim, H. D., & Tan, L. (2018). Advances in Fluid Dynamics of Turbomachinery. *International Journal of Rotating Machinery*, 2018.

https://doi.org/10.1155/2018/5747034
[6] Verses, J. P. (1992). A Survey of Instabilities Within Centrifugal Pumps and Concepts for Improving the Flow Range of Pump in Rocket Engines. *NASA Technical Memorandum 105439*, Lewis Research Centre, Cleveland, Ohio. https://ntrs.nasa.gov/citations/19920009038
[7] Arakaki, V. M. (2017). *High speed centrifugal pump design for rocket engine.* Thesis, Institute of Electrical and Electronics Engineering.
[8] Haidn, O. J. (2008). Advanced Rocket Engines. *Institute of Space Propulsion*, German Aerospace Centre (DLR). http://www.rto.nato.int
[9] Yoo, Y. J. & Lee, H. J. (2019). Influence of Fuel Boiling Point on Discharge Characteristics of Superheated Hydrocarbon Liquid Jets. *International Journal of Aeronautical and Space Sciences*, *21*, 186-200. https://doi.org/10.1007/s42405-019-00214-0
[10] Mishra, A. & Ghosh, P. (2017). Effect of leading edge sweep on the performance of cavitating inducer of LOX booster turbopump used in semicryogenic engine. *IOP Conf. Series: Materials Science and Engineering*, *171*. https://doi.org/10.1088/1757-899X/171/1/012062
[11] Tran, C., Ji, B., & Long, X. (2019). Simulation and Analysis of Cavitating Flow in the Draft Tube of the Francis Turbine with Splitter Blades at Off-Design Condition. *Technical Gazette*, *26*(6), 1650-1657. https://doi.org/10.17559/TV-20190316042929
[12] Boué, Y., Vinet, P., Magniant, S., Motomura, T., Blasi, R. & Dutheil, J. P. (2018). LOX/ methane reusable rocket propulsion at reach with large demonstrators tested. *Acta Astronautica*, 152, 542-556. https://doi.org/10.1016/j.actaastro.2018.06.018
[13] Greitzer, E. M. (1981). The Stability of Pumping Systems. *ASME Journal of Fluids Engineering*, 103, 193-242. https://doi.org/10.1115/1.3241725
[14] Kim, D. J., Sung, H. J., Choi, C. H., & Kim, J. S. (2017). Cavitation instabilities of an inducer in a cryogenic pump. *Acta Astronautica*, 132, 19-24. https://doi.org/10.1016/j.actaastro.2016.12.007
[15] Whitacker, L. H. L., Tomita, J. T., &Bringhenti, C. (2017). An evaluation of the tip clearance effects on turbine efficiency for space propulsion applications considering liquid rocket engine using turbopumps. *Aerospace Science and Technology*, 70, 55-65. https://doi.org/10.1016/j.ast.2017.07.038
[16] Mihalić, T., Medić, S., & Kondić, Z. (2013). Improving centrifugal pump by adding vortex rotor. *Technical Gazette*, *20*(2), 305-309. https://hrcak.srce.hr/en/clanak/147714
[17] Borse, S. L. (2014). CFD for Centrifugal Pump. *National Level Industry Institute Symposium on Turbomachines*, MNNIT, Allahabad, India. Retrieved from https://www.researchgate.net/publication/324602218_CFD_FOR_CENTRIFUGAL_PUMP
[18] Petit, O. & Nilsson, H. (2013). Numerical Investigations of Unsteady Flow in a Centrifugal Pump with a Vaned Diffuser. *International Journal of Rotating Machinery*, 2013. https://doi.org/10.1155/2013/961580
[19] Dixon, S. L. & Hall, C. A. (2014). *Fluid Mechanics and Thermodynamics of Turbomachinery.* Butterworth-Heinemann, Oxford.
[20] Pei, J., Yin, T., Yuan, S., Wang, W., & Wang, J. (2017). Cavitation optimization for a centrifugal pump impeller by using orthogonal design of experiment. *Chinese Journal of Mechanical Engineering*, *30*, 103-109. https://doi.org/10.3901/CJME.2016.1024.125
[21] Japikse, D. & Baines, N. C. (1997). *Introduction to Turbomachinery.* Concepts ETI Inc. & Oxford University Press, Oxford.
[22] Dragan, V. (2014). Aerodynamic reconfiguration and multicriterial optimization of centrifugal compressors - A case study. *INCAS Bulletin*, 6. https://doi.org/10.13111/2066-8201.2014.6.4.4
[23] Gherman, B., Silivestru, V., & Draghici, M. (2012). Aerodynamic Geometry optimization of a centrifugal Blower. *Polytechnic University of Bucharest Scientific Bulletin Series D: Mechanical Engineering*, *74*(1), 67-72. https://www.scientificbulletin.upb.ro/rev_docs_arhiva/fullff7_879496.pdf
[24] Dragan, V. (2017). Centrifugal compressor efficiency calculation with heat transfer. *IIUM Engineering Journal*, *18*(2), 225-237. https://journals.iium.edu.my/ejournal/index.php/iiumej/article/view/695
[25] Bistrian, D. A. (2014). A solution of the parabolized Navier–Stokes stability model in discrete space by two-directional differential quadrature and application to swirl intense flows. *Computers & Mathematics with Applications, 63*(3), 197-211. https://doi.org/10.1016/j.camwa.2014.05.017
[26] Liu, H. L., Liu, D. X., Wang Y., Wu, X. F., & Wang, J. (2013). Application of modified k-ω model to predicting cavitating flow in centrifugal pump. *Water Science and Engineering*, *6*(3), 331-339. http://dx.doi.org/10.3882/j.issn.1674-2370.2013.03.009
[27] Malael, I., Dumitrescu, H., & Dumitrache, A. (2011). Methods for improve the performance of the turbomachines using the flow control. *AIP Conference Proceedings*, *1389*(1), 1515-1519. https://doi.org/10.1063/1.3637913

Contact information:

Malael ION, Senior Researcher PhD
(Corresponding author)
National Research and Development Institute for Gas Turbines COMOTI
220 D Iuliu Maniu Bd., sector 6, cod 061126, OP 76, CP174
Bucharest, Romania
E-mail: ion.malael@comoti.ro

Bucur IOANA, Scientific Researcher BSc
National Research and Development Institute for Gas Turbines COMOTI
220 D Iuliu Maniu Bd., sector 6, cod 061126, OP 76, CP174
Bucharest, Romania
E-mail: ioana.bucur@comoti.ro